Journal of Structural Chemistry. Vol. 57, No. 7, pp. 1429-1435, 2016.

ANALYSIS OF THE ATOMIC STRUCTURE OF COLLOIDAL QUANTUM DOTS OF THE CdSe FAMILY: X-RAY SPECTRAL DIAGNOSTICS AND COMPUTER MODELLING

I. A. Pankin[1], A. N. Kravtsova[1]*,
O. E. Polozhentsev[1], A. L. Trigub[2],
M. A. Soldatov[1], and A. V. Soldatov[1]

UDC 539.2

Colloidal quantum dots of the CdSe family have been studied by X-ray absorption near edge structure (XANES) spectroscopy and computer modelling. Cd*K* edge XANES spectra in colloidal quantum dots based on varisized CdSe nanoparticles have been recorded. Atomic structure of CdSe particles and also CdSe particles doped by transition metal atoms Mn and Co has been modelled based on the density functional theory. The embedding of the doping atoms is shown to result in considerable changes in the local atomic structure of CdSe particles. XANES spectra have been calculated above the Cd*K* edge in CdSe particles, above the Mn*K* edge in CdSe:Mn particles, above the Co*K* edge in CdSe:Co particles. The sensitivity of XANES spectroscopy to small changes in structural parameters of the nanoparticles of CdSe family has been demonstrated that furnishes an opportunity to apply it for the verification of atomic structure parameters around positions of cadmium and doping atoms of transition metals in quantum dots based on CdSe.

DOI: 10.1134/S0022476616070180

Keywords: quantum dots, cadmium selenide, doping, local atomic structure, XANES spectroscopy, computer modelling, density functional theory.

INTRODUCTION

Quantum dots (QD) attract considerable attention of the researchers due to their unique optical and electronic properties [1-5]. The unique properties of QD are attractive for various applications in optical [1, 2] and electronic devices [3, 4] including transistors, materials for solar cells, components of super-fast switches, logical circuits and quantum computers. QD can be also used for various biomedical applications: visualization [6, 7], therapy of oncological diseases [6, 7] and as biosensors [8, 9].

QD comprise semiconductor nanoparticles which have electronic properties intermediate between bulk material and discrete molecules that is connected with a manifestation of the quantum effect [10]. The width of the band gap of QD depends on their size and chemical composition. Doping is one of the methods of the influence on QD properties [11, 12]. It was shown [12, 13] that the substitution of semiconductor cations by 3*d* transition metal atoms and rare-earth elements brings into existence of magnetic properties that considerably extends the fields of application of QD.

[1]International Research Center "Smart Materials", Southern Federal University, Rostov-on-Don, Russia; *akravtsova@sfedu.ru. [2]National Research Center "Kurchatov Institute", Moscow, Russia. Translated from *Zhurnal Strukturnoi Khimii*, Vol. 57, No. 7, pp. 1508-1514, September-October, 2016. Original article submitted December 30, 2015; revised March 29, 2016.

Previously it was studied QD based on CdSe doped by 3*d* transition metal atoms such as Cr [12], Mn [11, 13, 14], Co [11], Fe [11, 15]. Kwak et al. [16] showed that the width of the band gap and the wavelength of the fluorescence in CdSe nanocrystals with zinc blende structure can be regulated with doping by Mg atoms (<9.8 at.%). The optical properties of QD can be changed depending on the concentration of doping elements [17] and positions of impurity atoms [18]. The questions of positions of doping atoms in CdSe structure, determination of local atomic structure and electronic structure parameters, and the influence of the impurity atoms on the band gap width and magnetic characteristics of QD remain important. One of the methods allowing investigation of local atomic and electronic structure of materials is X-ray Absorption Near Edge Structure (XANES) spectroscopy [19], which is sensitive to the oxidation state of an absorbing element and the local atomic structure around the selected type of atoms. The analysis of X-ray absorption spectra and computer modelling allow investigating the electronic structure of the material under study. Before, the possibility of application of XANES spectroscopy for studies of QD of the CdS [20] and CdTe [21] families was demonstrated.

In the present work the atomic and electronic structure of QD of the CdSe family has been studied by XANES spectroscopy and computer modelling based on density functional theory (DFT). Cd*K*-XANES spectra in colloidal QD based on varisized CdSe nanoparticles have been measured. The results of the optimization of the atomic structure of CdSe clusters and CdSe doped by the Mn and Co transition metal atoms have been presented. The sensitivity of XANES spectroscopy for the verification of the local atomic structure of QD of the CdSe family obtained in the result of computer modelling has been demonstrated.

EXPERIMENTAL

In the work commercial samples of colloidal QD based on CdSe produced by Sigma Aldrich were studied. The samples represented colloidal solutions of cadmium selenide CdSe in toluene. The concentration of the colloidal solution of CdSe QD was 5 mg/ml. According to the certificate of the samples, the sizes of the investigated particles lay in the ranges 2.1-2.3 nm, 2.6-2.8 nm and 6.2-7.7 nm with the corresponding wavelengths of a fluorescence in the optical diapason λ = 480 nm, 520 nm and 640 nm.

XANES spectra above the Cd*K* edge (E_{1s} = 26711 eV) of colloidal QD based on CdSe were measured at the Structural Materials Science (STM) beamline of the synchrotron radiation source at NRC "Kurchatov Institute". The optical scheme of the station (a system of monoblock monochromators and collimating slits) allows the energy of the incident radiation to be varied in the diapason from 4.9 keV to 35 keV. The energy resolution ($\Delta E/E$) of the STM beamline is $2 \cdot 10^{-4}$. The density of the photon flux on the sample was $5 \cdot 10^{7}$ photon/(s·mm^2) at the storage ring current 100 mA. The measurements were carried out in transmission mode. With the aim of increasing the signal-to-noise ratio, the peculiarities of the measuring technique of X-ray absorption spectra for liquid diluted samples were taken into account. The optical path length of X-ray radiation in the sample was ~15 mm using special cylindrical capillaries. Gas-filled argon cameras equipped by picoamperemeters were used as detectors of the intensity of the incident radiation on the sample and the radiation transmitted through the sample. The Cd *K*-XANES spectra in the CdSe QD obtained in the result of averaging over several runs were calibrated in the energy scale and normalized to unity.

CALCULATION METHOD

The atomic structure optimization of semiconducting QD based on cadmium selenide nanoparticles was carried out using the VASP 5.3 (Vienna *Ab initio* Simulation Package) software code [22]. Calculations in the VASP 5.3 software package are realized based on DFT using periodical boundary conditions and the pseudopotential approximation that enables the resource capacity of calculation tasks to be considerably decreased.

The pseudopotentials of the PAW-PBE type (projector augmented-wave Perdew–Burke–Ernzerhof) [23] were used to model quantum dot structure. Self-Consistent Field (SCF) cycles of an electronic density were calculated using Dawson functions. The energy criterion of the convergence of cycles of an ion relaxation was $1.5 \cdot 10^{-4}$ eV. The calculations of the electronic structure of CdSe, CdSe:Mn, CdSe:Co clusters were performed taking into account the presence of the

uncompensated magnetic moment in transition metals Mn, Co, Cd. The basis set of plane waves restricted the energy to 400 eV for the CdSe cluster and 450 eV for the clusters with impurity atoms CdSe:Mn and CdSe:Co.

Spherical fragments of the crystalline solid CdSe [24] were used as an initial structure of QD based on CdSe preceding optimization. Spherical fragments of CdSe with the central cadmium atom substituted by Co and Mn atoms were used as initial structures for the optimization of QD based on CdSe doped by the transition metals Co and Mn, correspondingly. The modelling of the CdSe QD structure was carried out for the clusters of 7 Å radius consisting of 48 atoms. Because the calculations in the VASP 5.3 software code is realized using the periodical boundary conditions, the particles CdSe and CdSe doped by Mn and Co were placed in the cell with the parameter a = 22 Å to exclude an interaction of the nanoparticles relating to the neighboring cells.

The VASP 5.3 code is designed for the modelling of the atomic and electronic structure of periodical systems in the framework of the ground state of an electronic system, whereas the consideration of a core hole created by an electron transition is necessary for the correct description of X-ray absorption spectra above *K* edges of metals [25]. Because of this, the calculations of the X-ray absorption near-edge structure spectra were performed taking into account the core hole on the basis of the full-potential finite difference method realized in the FDMNES software code [26]. The finite difference method is a widely known method for the numerical solution of differential equations where the solution of Schrödinger equation is sought on the discrete grid of points. A recently updated version of the FDMNES software [26] was used which allows the computational capacity of full-potential calculations of X-ray absorption spectra to be considerably reduced using Sparce Solvers in the process of the diagonalization of the finite difference matrix. The calculations of XANES spectra were carried out using the exchange-correlation potential of Hedin–Lundquist type.

Because FDMNES code allows to perform non-self-consistent calculations, the calculations of the partial densities of states (DOS) near the conduction band bottom and valence band top of the CdSe, CdSe:Mn, CdSe:Co clusters were performed based on the self-consistent full multiple scattering method in real space realized in the FEFF8.4 code [27].

Structure optimization of quantum dot based on CdSe and X-ray absorption spectra calculations were carried out using the supercomputer “Blokhin” at IRC “Smart materials” of Southern Federal University.

RESULTS AND DISCUSSION

The Cd*K* edge XANES spectra were recorded for commercial samples of CdSe QD produced by Sigma Aldrich (see Experimental part). The measurements were performed in transmission mode. To increase the signal-to-noise ratio, we placed a liquid sample in a narrow capillary of cylindrical shape. The cylindrical capillary was mounted on a sample holder so that the X-ray beam falls onto the sample axially that allows increasing the optical path length in the sample to 15 mm.

Fig. 1 presents the experimental Cd*K*-XANES spectra of varisized colloidal CdSe QD in comparison to the theoretically calculated spectrum for bulk CdSe. The experimental Cd*K*-XANES spectra measured for the particles of different sizes have a similar fine structure that testifies the similar local atomic structure around the cadmium positions in the QD under study. With decreasing particles size, the increase of the energy distance between the spectral features indicated as *A* and *B* is observed that according to Natoli’s rule can testify that the interatomic distances in the QD samples under study are decreased with decreasing particles size. One can see that the theoretical spectrum for the bulk sample is well agreed with the experimental spectrum for QD of the largest size (6.2-7.7 nm) in the energy positions of the maxima.

In the following step the optimization of the geometrical atomic structure of the cadmium selenide particle was performed. A spherical fragment of crystalline CdSe of wurtzite phase [24] of 7 Å radius comprising 19 atoms of Cd and 29 atoms of Se (Fig. 2*a*) is used as an initial structure of the particle. In the crystal structure of CdSe the Cd atoms are coordinated by four Se atoms. The Cd–Se distances are 2.630-2.632 Å. According to the results of the geometry optimization (Fig. 2*b*) the local environment of the central atom of the cluster is insignificantly changed. Four Se atoms are located in the first coordination sphere of the central Cd atom. The Cd–Se interatomic distances lie in the range of 2.630-2.704 Å. So, it was shown that for atomic clusters of small size (to 1 nm) CdSe holds the structure and interatomic distances corresponding to the values of the bond lengths in bulk solid cadmium selenide.

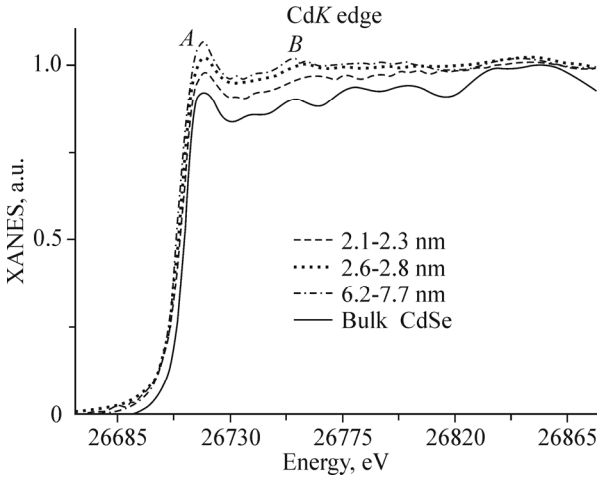

Fig. 1. Experimental Cd*K* edge XANES spectra in colloidal QD CdSe of different sizes (2.2-2.3 nm, 2.6-2.8 nm, 6.2-7.7 nm). Theoretical Cd*K* edge XANES spectrum of bulk CdSe is also presented.

The calculations of the Cd*K*-XANES spectra for the initial and optimized structures of CdSe clusters were performed based on the full potential finite difference method (Fig. 3). One can see that XANES spectra are sensitive to the minor changes of the interatomic distances in small CdSe particles.

In the following step the optimization of the structure of CdSe particles doped by transition metals Mn and Co was performed. Spherical fragments of solid CdSe [24] with the central Cd atom substituted by Mn or Co were used as initial structures preceding the optimization. The spherical clusters of 7 Å radius comprising 18 Cd atoms, one impurity atom (Mn or Co) and 29 Se atoms were considered for modelling the structure of the doped CdSe particles. Fig. 4 presents the images of the structures of atomic clusters CdSe:Mn (*a*) and CdSe:Co (*b*) obtained in the result of the optimization.

In the result of the embedding of the transition metal and the following optimization of the atomic cluster geometry, the structural changes are observed in the local surroundings of the impurity atoms and in the structure of the cluster as a whole. Table 1 presents the changes in interatomic distances for the nearest coordination of the central atom of the cluster in the result of the optimization of the atomic structure.

The Mn*K* edge and Co*K* edge XANES spectra have been calculated for the initial and optimized structures of the CdSe:Mn and CdSe:Co particles, correspondingly. Figs. 5 and 6 show the calculated XANES spectra. In Figs. 5, 6 one can see that the Mn*K*- and Co*K*-XANES spectra in the CdSe:Mn and CdSe:Co particles, correspondingly, are sensitive to the changes of the atomic structure of the particles as the spectra calculated for the non-optimized and optimized geometries

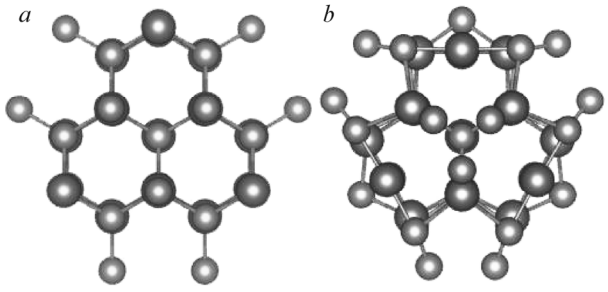

Fig. 2. Structure of the CdSe particle with a 7 Å radius before the optimization (*a*) and after the optimization (*b*).

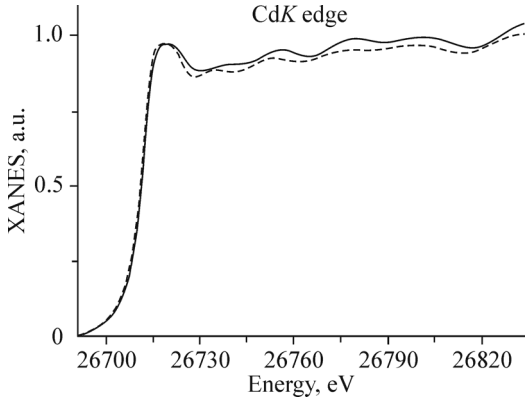

Fig. 3. Theoretical Cd*K* edge XANES spectra in the 7 Å CdSe nanoparticle. The spectrum calculated for the initial structure is shown by solid line and that for the optimized structure is shown by dotted line.

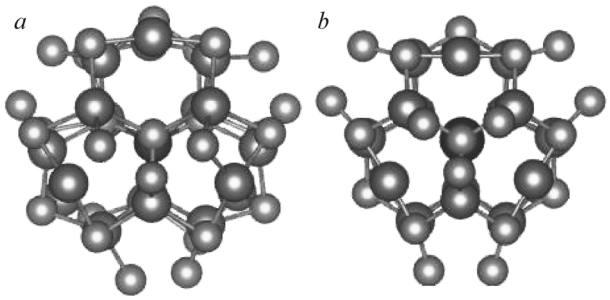

Fig. 4. Images of optimized CdSe nanoparticle structures doped by Mn (*a*) and Co (*b*).

show considerable distinctions in the energy position of the spectral features and in its relative intensity. Consequently, XANES spectroscopy can be used for the verification of local atomic structure parameters around positions of doping transition metal atoms in QD of the CdSe family obtained in the result of a computer modelling.

With the aim of the study of the electronic structure of QD based on CdSe, the calculations of the partial DOS near the valence band top and the conduction band bottom were carried out for the model of a monatomic defect of substitution of Cd atom by Mn, Co atoms in the crystalline phase of cadmium selenide CdSe [24]. The calculations were performed in the ground state of the electronic system using the FEFF8.4 code. The top of the valence band of semiconducting CdSe is formed due to the hybridized Se *p* and Cd *p*, *d* states (Fig. 7). The bottom of the conduction band of the semiconducting CdSe is formed due to the hybridized Se(*s*,*p*) and Cd(*s*,*p*,*d*) states.

Under doping of CdSe semiconductor by Mn atoms the impurity levels appear in the band gap, which correspond to the hybridized Mn *d* and Se *p* states. So, the top of the valence band of the doped semiconductor CdSe:Mn is formed due to

TABLE 1. Structural Parameters of Particles Based on CdSe Obtained as a Result of the Geometrical Optimization Based on DFT Using VASP 5.3 Code

Parameter	Crystal CdSe		Cluster R = 7 Å CdSe		Cluster R = 7 Å CdSe:Mn		Cluster R = 7 Å CdSe:Co	
Bond type	Cd–Se	Cd–Cd	Cd–Se	Cd–Cd	Mn–Se	Mn–Cd	Co–Se	Co–Cd
Average interatomic distance, Å	2.6317	4.2976	2.6495	4.4263	2.3506	4.1880	2.2763	3.9284
Mean root square deviation, Å	0.0006	0.0009	0.0195	0.1391	0.1637	0.1243	0.0314	0.0323

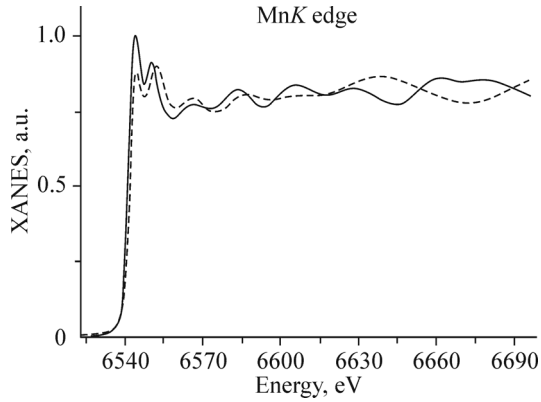

Fig. 5. Theoretical Mn*K* edge XANES spectra calculated for the initial structure of the CdSe:Mn particle with a 7 Å radius (solid line) and the structure obtained as a result of the optimization (dotted line).

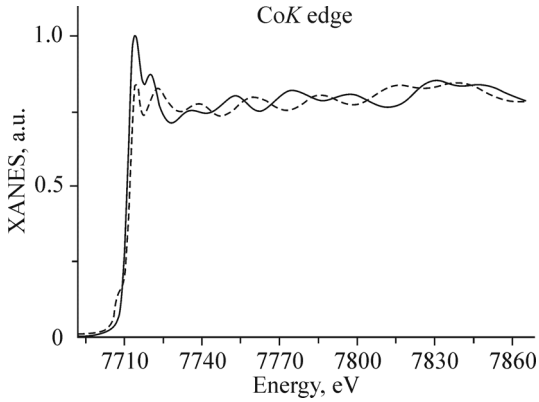

Fig. 6. Theoretical Co*K* edge XANES spectra calculated for the initial structure of the CdSe:Co particle with a 7 Å radius (solid line) and the structure obtained as a result of the optimization (dotted line).

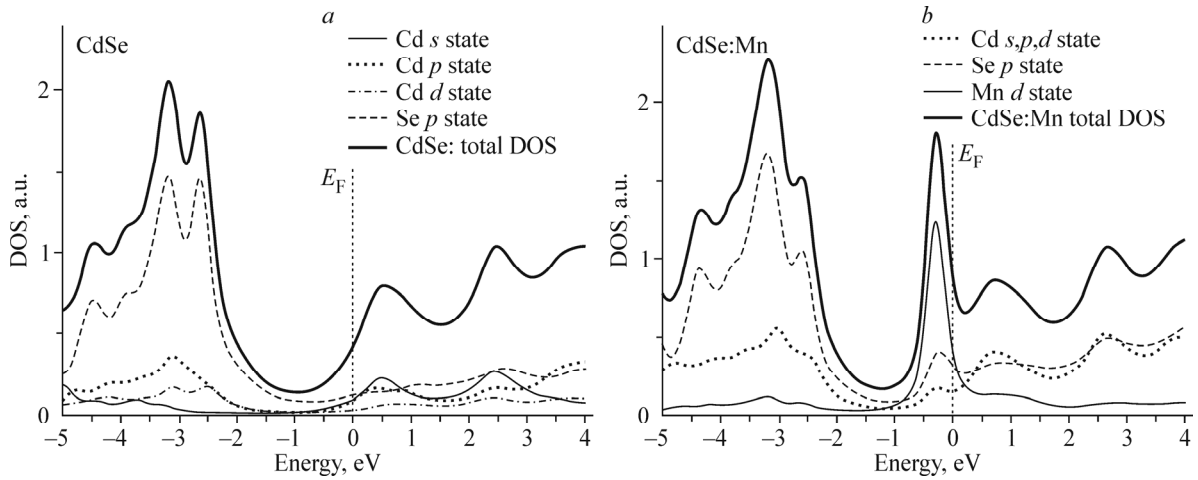

Fig. 7. Total and partial densities of states near the top of the valence band and the bottom of the conduction band of CdSe (*a*) and CdSe doped with manganese (*b*).

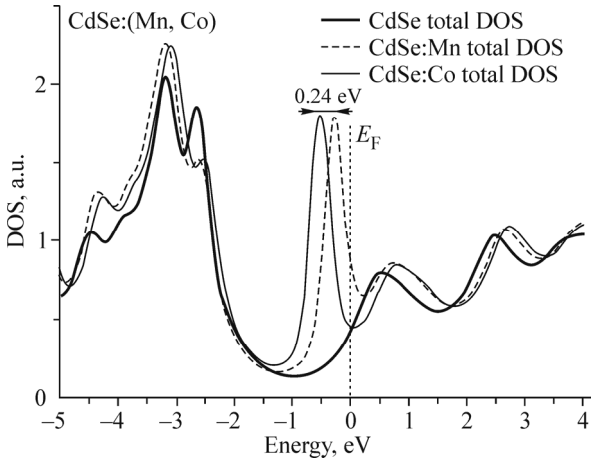

Fig. 8. Total densities of states near the top of the valence band and the bottom of the conduction band of CdSe and CdSe:Mn, CdSe:Co.

the Mn *d* and Se *p* states. Under doping by Co, the top of the valence band of the doped CdSe:Co is formed due to the hybridization of the Co *d* and Se *p* states, correspondingly. Fig. 8 presents the total density of states near the top of the valence band and the bottom of the conduction band of CdSe and doped by manganese and cobalt CdSe:(Mn, Co). The bottom of the conduction band of the doped CdSe:(Mn, Co) is formed due to the hybridization of the Se(*s*,*p*), Mn(*d*) and Cd(*s*,*p*,*d*) states. It is traced the tendency of the displacement of the electronic levels corresponding to the hybridized *d* states of the doping metals of transition elements and the Se *p* states to the lower energies for the doping atoms with a high number *Z*. The calculated densities of electronic states allows the size of the band gap to be semiquantatively estimated. The semiquantative character of data is conditioned by that fact that the densities of electronic states calculated by the full multiple scattering, as a rule, lack the features, which may obtain using band methods, however, in most cases the obtained resolution is sufficient for a comparison with experimental data [29]. Overall, the doping by transition metal atoms can significantly influence on the electronic structure of QD.

CONCLUSIONS

QD doped by transition metal atoms combine the unique magnetic and optical properties and considerably extend the capability of their application. In the work the atomic and electronic structure of colloidal QD of the CdSe family have

been studied by the computer modelling based on DFT and XANES spectroscopy. The Cd*K* edge XANES in colloidal CdSe QD of different sizes were measured at NRC "Kurchatov Institute". It have been performed the optimization of the atomic structure of CdSe nanoparticles and CdSe doped by transition metal atoms (Mn, Co) based on DFT using the VASP 5.3 code. The results of the optimization show that the doping of CdSe particles by manganese and cobalt leads to the significant changes in the atomic structure of the particles. XANES spectra above the Cd *K* edge in CdSe particles, above the Mn*K* edge in CdSe:Mn particles and above the Co*K* edge in CdSe:Co particles have been calculated. The modelling of XANES spectra showed the distinction in the fine structure of X-ray absorption spectra calculated for the structural models of CdSe, CdSe:Mn and CdSe:Co particles taking into account and without considering the optimization of their atomic geometry. The sensitivity of XANES spectroscopy to small changes of structural parameters of the particles based on CdSe shows the potentials for its application as one of the basic methods for the diagnostics of the local atomic structure of colloidal QD of the CdSe family including ones doped by transition metal elements.

The research was supported by the Ministry of Education and Science grant "Computer nanodesign, synthesis and diagnostics of quantum nanostructures", project part of government task N 16.148.2014/K, number of state registration 114072270020.

REFERENCES

1. G. Konstantatos, I. Howard, A. Fischer, et al., *Nature*, **442**, 180 (2006).
2. L. Huang, C.-C. Tu, and L. Y. Lin, *Appl. Phys. Lett*., **98**, 113110 (2011).
3. L. Li, A. Pandey, D. J. Werder, et al., *J. Am. Chem. Soc*., **133**, 1176 (2011).
4. L. Qian, Y. Zheng, J. Xue, and P. H. Holloway, *Nat. Photonics*, **5**, 543 (2011).
5. J. M. Klostranec and W. C. Chan, *Adv. Mater*., **18**, 1953 (2006).
6. L. Shao, Y. Gao, and F. Yan, *Sensors*, **11**, 11736 (2011).
7. L. Liu, Q. Miao, and G. Liang, *Materials*, **6**, 483 (2013).
8. A. J. Haes, W. P. Hall, L. Chang, et al., *Nano Lett*., **4**, No. 6, 1029 (2004).
9. I. L. Medintz, H. T. Uyeda, E. R. Goldman, and H. Mattoussi, *Nat. Mater*., **4**, 435 (2005).
10. A. D. Yoffe, *Adv. Phys*., **50**, 1-208 (2001).
11. A. Alsaad, *Physica B*, **440**, 1 (2014).
12. Y.-H. Zheng, J.-H. Zhao, and J.-F. Bi, et al., *Chin. Phys. Lett*., **24**, 2118 (2007).
13. L. G. Gutsev, N. S. Dalal, and G. L. Gutsev, *Comput. Mater. Sci*., **83**, 261 (2014).
14. S. K. Shinde, D. P. Dubal, G. S. Ghodake, and V. J. Fulari, *J. Electroanal. Chem*., **727**, 179 (2014).
15. S. Arif, B. Amin, I. Ahmad, et al., *Curr. Appl. Phys*., **12**, 184 (2012).
16. W.-C. Kwak, T. G. Kim, W.-S. Chae, and Y.-M. Sung, *Nanotechnology*, **18**, 205702 (2007).
17. H. S. Yang, S. Santra, and P. H. Holloway, *J. Nanosci. Nanotechnol*., **5**, 1364 (2005).
18. Y. A. Yang, O. Chen, A. Angerhofer, and Y. C. Cao, *J. Am. Chem. Soc*., **128**, 12428 (2006).
19. G. Bunker, *Introduction to XAFS. A Practical Guide to X-Ray Absorption Fine Structure Spectroscopy*, University Press, UK, Cambridge (2010).
20. A. N. Kravtsova, A. V. Soldatov, S. A. Suchkova, et al., *J. Struct. Chem*., **56**, 517 (2015).
21. A. N. Kravtsova, K. A. Lomachenko, S. A. Suchkova, et al., *Izv. Ross. Akad. Nauk, Ser. Fiz*., **79**, 1615 (2015).
22. G. Kresse and J. Furthmüller, *Comput. Mater. Sci*., **6**, 15 (1996).
23. J. P. Perdew, K. Burke, and M. Ernzerhof, *Phys. Rev. Lett*., **77**, 3865 (1996).
24. Y.-N. Xu and W. Y. Ching, *Phys. Rev. B*, **48**, 4335 (1993).
25. H. Modrow, S. Bucher, J. J. Rehr, and A. I. Ankudinov, *Phys. Rev. B*, **67**, 035123 (2002).
26. Y. Joly, *Phys. Rev. B*, **63**, 125120 (2001).
27. S. A. Guda, A. A. Guda, M. A. Soldatov, et al., *J. Chem. Theor. Comput*., **11**, 4512 (2015).
28. A. L. Ankudinov, B. Ravel, J. J. Rehr, and S. D. Conradson, *Phys. Rev. B*, **58**, 7565 (1998).
29. M. S. Moreno, K. Jorissen, and J. J. Rehr, *Micron*, **38**, 1-11 (2007).